

Cite this: *Phys. Chem. Chem. Phys.*, 2011, **13**, 8422–8432

www.rsc.org/pccp

PAPER

A portable intermolecular potential for molecular dynamics studies of NMA–NMA and NMA–H₂O aggregates

M. Albertí,^{*a} N. Faginas Lago,^b A. Laganà^b and F. Pirani^b

Received 9th September 2010, Accepted 24th January 2011

DOI: 10.1039/c0cp01763a

A recently formulated intermolecular potential has been adapted to describe the interaction of the *N*-methylacetamide (NMA) dimer and of the NMA–H₂O adduct. The pure electrostatic component of the intermolecular potential functional representation is as usual expressed in terms of a set of punctual charges distributed over the molecular frames, consistently with the permanent molecular dipole values. In contrast, the remainder of the intermolecular potential is expressed in terms of Improved Lennard Jones effective pair potential functions, referred to multiple interaction centers (or sites) placed on the *N*-methylacetamide molecule and to a single interaction center placed on the water molecule. The characteristic of this pair potential relies on a mix of transferable and non-transferable descriptions of the parameters. The first set of parameters has a structural connotation bearing a site–site interaction nature and exploiting the molecular polarizability decomposability. The second one, depending on the particles clustering and charge distribution and transfer, bears a delocalized and ambient bulk nature. This choice has been tested against *ab initio* calculations and molecular dynamics simulations. The results show that the model potential is appropriate for describing the energetic of the various stable configurations of NMA–NMA and NMA–H₂O weakly interacting aggregates, including the formation of hydrogen bonds.

1. Introduction

The *N*-methylacetamide (NMA) has been, in the fairly recent past, extensively studied from both theoretical and experimental points of view and has been considered as a model useful for the investigation of larger molecules containing the peptide group. As a matter of fact, starting from the year 1964,¹ the investigation of the inter-peptide and peptide–solvent interactions has often been carried out by studying the NMA–NMA and the NMA–H₂O systems, respectively. In particular, the behaviour of the amide functional group in *N*-methylacetamide has been investigated experimentally^{2–8} as well as theoretically^{9–16} both to obtain structural information on the NMA dimer and to understand the dynamics of the related hydrogen bonding. As to the NMA–H₂O complex, its analysis has been performed using both *ab initio* and molecular dynamics (MD) methods (see for instance ref. 17) with the purpose of making it a case study for the formation of hydrates in which water can act as an electron-acceptor from the carbonyl group and as an electron-donor to the amide group. As a matter of fact, the H-bonds formed either between the oxygen of the carbonyl group of NMA and any hydrogen atom of the water molecule or between the oxygen atom of water and the H atom of the

N–H bond (as well as the N–H···O=C and the C–H···O=C ones formed by the NMA dimers) offer an important example of the role that this type of bond plays in stabilizing intermolecular aggregates.^{9,18,19}

This makes of fundamental importance the development of an appropriate transferable description of the intermolecular interaction. Obviously, by definition, the only strictly speaking transferable approach to the description of the intermolecular interaction is the high level *ab initio* one. Unfortunately, for the systems considered here, high level *ab initio* calculations are computationally so demanding that an adequate investigation of the full configuration space is still, in practice, out of reach. For this reason, high level *ab initio* calculations are usually confined to the most stable geometries of the monomers (the so called strong or intramolecular interaction region) and are seldom extended to molecule–molecule (the so called weak or intermolecular) interaction regions, which are often governed by long range non-covalent forces. In this paper the popular alternative approach of adopting a semiempirical functional form has been chosen. For this purpose we consider in the paper a recently proposed semiempirical transferable model potential allowing a proper balance between structural and environmental (including the formation of H-bonds) contributions and we apply it to the NMA–NMA and the NMA–H₂O aggregates.

Accordingly the paper is structured as follows: in Section 2 the formulation of the semiempirical model potential is

^a IQTCUB, Departament de Química Física, Universitat de Barcelona, Barcelona, Spain. E-mail: m.alberti@ub.edu

^b Dipartimento di Chimica, Università di Perugia, Perugia, Italy

outlined, in Section 3 the MD calculations on the NMA dimer are illustrated, in Section 4, we discuss the portability of the proposed model potential to other MD calculations. Concluding remarks are given in Section 5.

2. The formulation of the intermolecular interaction

As usual in semiempirical approaches the total interaction is formulated as a sum of an intra- (V_{intra}) and an inter- (V_{inter}) molecular term. Following the guidelines of the work performed in the past^{20–23} for the NMA V_{intra} we adopted the AMBER parameterization,²⁴ while for the H₂O one we adopted that of the non-rigid molecule of ref. 25 and 26. For V_{inter} we split the interaction into a V_{el} (pure electrostatic) and a V_{vdW} (van der Waals) component (in the past often called, V_{nel}).²⁷

$$V_{\text{inter}} = V_{\text{el}} + V_{\text{vdW}} \quad (1)$$

which are represented by means of suitable analytical functions involving a few parameters linked to some physical properties. In the case of the NMA–NMA and NMA–H₂O aggregates considered in this paper in order to build a suitable V_{inter} and to evaluate related properties the trans-NMA conformer is considered because this is the most abundant and stable monomer²⁸ of the two that have been experimentally detected.²⁹

2.1 The van der Waals component

V_{vdW} is an effective potential that explicitly considers a certain number of interaction centers (depending on the complexity of the considered molecules) placed on some of their atoms (or groups of atoms) and incorporates as well exchange (size) and dispersion contributions. As we shall discuss later in more detail, here V_{vdW} implicitly includes also induction, charge transfer and other contributions to the intermolecular interaction. Five effective interaction centers were found to be sufficient for NMA. In particular, two of such centers are associated with the CH₃ groups and were placed on the related C (C_R and C_L in Fig. 1) atoms. Two other interaction centers are associated with (and placed on) the C and O atoms of the carbonyl group (C and O in Fig. 1). The last interaction center was associated with the NH group and the related lone pair, and was placed on the N atom (N in Fig. 1). A polarizability contribution, whose sum reproduces the value of the molecular polarizability, was assigned to each center (see Table 2). The case of the H₂O molecule, instead, turned out to be much

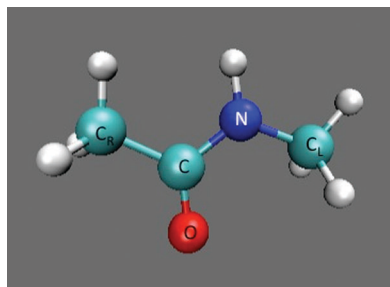


Fig. 1 The NMA trans molecule and the location of the dispersion centers considered (see text).

simpler because a single average center placed on the O atom (Ow) and including the effect of two OH bonds and two lone pairs was considered. The choice of using a single average center for water coincides with the recent proposal of the AMPF model potential of water^{26,30–32} that has been successfully used to predict the main properties of (liquid and small clusters) water derived from both the experiments and the *ab initio* calculations. Accordingly, for NMA–NMA and the NMA–H₂O, V_{vdW} is expressed as a sum of 15 and 5 effective pairs of interactions, respectively, with each effective pair contribution being represented by an Improved Lennard Jones (V_{ILJ}) functional form,^{33,34} as follows:

$$V_{\text{ILJ}}(r) = \varepsilon \left[\frac{m}{n(r) - m} \left(\frac{r_0}{r} \right)^{n(r)} - \frac{n(r)}{n(r) - m} \left(\frac{r_0}{r} \right)^m \right]. \quad (2)$$

In eqn (2), ε , r_0 and m are pair specific consistent parameters while r is the distance between the two centers. The first term of the bracketed sum in eqn (2) (the positive one) represents the size-repulsion contribution arising from each pair, while the second term (the negative one) represents the effective dispersion attraction ascribable to the same pair. The $n(r)$ exponent of the first term modulates the falloff of the repulsion as a function of r as follows:

$$n(r) = \beta + 4.0 \left(\frac{r}{r_0} \right)^2 \quad (3)$$

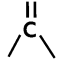

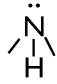
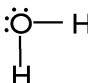
with β being an adjustable parameter that introduces the metric of a more ambient-like characteristic (that can be named as the hardness of the interacting partners^{33,34}) by modulating the repulsion and controlling the strength of the attraction. The introduction of this modulation (absent in V_{LJ}) provides V_{ILJ} with the possibility of indirectly taking into account induction, charge transfer and atom clustering effects. The additional parameter β of V_{ILJ} with respect to those of the usual Lennard Jones (V_{LJ}) potential corrects the dependence of the interaction on the internuclear distance, removing most of the V_{LJ} inadequacies in the asymptotic region.³⁴ This approach has already shown in the recent past to be portable to other types of clusters.^{26,27,31–43} This extra adaptability of V_{ILJ} allows the use of the same values of ε (the potential well depth) and r_0 (the equilibrium distance) for different molecules, if the same interaction centers are considered.⁴⁴ This assigns to ε and r_0 a structural meaning, while leaving to β the role of embodying in the pair interactions the contributions of more collective and ambient effects which will be used to drive an optimization procedure that will be further discussed later.

The values of ε and r_0 , adopted for NMA–NMA and NMA–H₂O, are given in Table 1, by adopting the same labeling of Fig. 1. In Table 1, the Ow symbol indicates the single H₂O average interaction center placed, as mentioned before, on the oxygen atom.^{30,32} As indicated above, the quoted values have been derived from the polarizabilities of atoms and from the effective group polarizabilities of CH₃, NH and H₂O (see Table 2), following the rules given in ref. 45. This choice guarantees the correct reproduction of molecular polarizabilities with the internal consistency of the parameters being guaranteed by the adopted procedure.

Table 1 The values of the well depth (ϵ), equilibrium distance (r_0) and m parameters for the NMA–NMA and NMA–H₂O interactions

NMA–NMA			
Pairs	ϵ/meV	$r_0/\text{\AA}$	m
C _R –C _R	12.64	3.952	6.0
C _R –C _L	12.64	3.952	6.0
C _L –C _L	12.64	3.952	6.0
C–C	6.52	3.628	6.0
O–O	5.16	3.398	6.0
N–N	9.12	3.773	6.0
C _R –C	8.81	3.805	6.0
C _L –C	8.81	3.805	6.0
C _R –O	7.28	3.721	6.0
C _L –O	7.28	3.721	6.0
C _R –N	10.64	3.867	6.0
C _L –N	10.64	3.867	6.0
C–O	5.64	3.521	6.0
C–N	7.66	3.704	6.0
O–N	7.51	3.670	6.0
NMA–H ₂ O			
C _R –O _w	10.560	3.850	6.0
C _L –O _w	10.560	3.850	6.0
C–O _w	7.66	3.683	6.0
O–O _w	6.58	3.584	6.0
N–O _w	9.10	3.754	6.0

Table 2 Polarizability values assigned to the interaction centers

Group	Polarizability/ \AA^3
–C _R H ₃	2.18
–C _L H ₃	2.18
	1.20
	0.76
	1.58
	1.47

2.2 The electrostatic component

V_{el} is formulated as usual, as a sum of coulombic potentials associated with a set of punctual charges localized on the atoms of the corresponding molecule having a defined spatial distribution. For H₂O two different charge distributions have been used, consistent with the dipole moments of the water molecule in the gas phase and of the water dimer.⁴⁶ The choice of the spatial distribution of the charge is not a problem for H₂O due to the dominant role of oxygen in that molecule, but this choice has instead a certain extent of arbitrariness for more complex systems⁴⁷ like NMA aggregates that can be stabilized as different isomers. Because of this, three different groups of punctual charges (though having the same location) have been used for NMA (AMBER,²⁰ CHARMM22²¹ and OPLS-AA).²² As apparent from Table 3 in which the characteristics of the different distributions are illustrated the variation

Table 3 Punctual charge distributions (a.u.) and dipole moments, μ (Debye)

	AMBER	CHARMM22	OPLS-AA
CR1	–0.2078	–0.2700	–0.1800
C1	0.5869	0.5100	0.5000
O	–0.5911	–0.5100	–0.5000
N	–0.4192	–0.4700	–0.5000
CL1	–0.0411	–0.1100	0.0200
HR1	0.0173	0.0900	0.0600
HR1	0.0173	0.0900	0.0600
HR1	0.0173	0.0900	0.0600
H	0.2823	0.3100	0.3000
HL1	0.1127	0.0900	0.0600
HL1	0.1127	0.0900	0.0600
HL1	0.1127	0.0900	0.0600
μ	5.567	5.240	4.726
O _w		–0.7572	
H _w		0.3786	
μ		2.10	
O _w		–0.6670	
H _w		0.3335	
μ		1.85	

of the charges (though not of their positions) has a marked impact on the dipole moment value.

Although the pure electrostatic component of the interaction is fully embodied in V_{el} , the way V_{ILJ} is formulated (see eqn (2) and (3)) makes it, as already mentioned, indirectly dependent on the charge distribution adopted for V_{el} . In fact, through βV_{ILJ} incorporates (in a parametric fashion) some contributions arising from the incomplete separability of the electrostatic and non-electrostatic components when formulated in terms of pair interactions. As a matter of fact, the value of β is sensible to the charge distribution and to the choice of the interaction of the reference centers. For example, the CH₃ groups can be represented either as a single pseudoatom using the polarizability in Table 2 or as a cluster of diatoms⁴⁵ corresponding to the associated chemical bonds whose polarizability values must sum to that of the pseudoatom.

As discussed in ref. 48, for the van der Waals interaction of small atoms and small molecules the initial β values can be estimated from the cubic root of the polarizability of the involved partners. Most often, however, due to the reasons stressed above and to coming into play of charge transfer effects (as is the case of H bonding), the values of β need to be varied within a well defined interval for optimization. For this reason in our study the β values obtained from the above mentioned procedure were used as starting points of a MD iterative optimization. In particular, in our work the value of β was optimized against the binding energy when different sets of punctual charge values were used.

3. The NMA–NMA molecular dynamics

The above mentioned optimization of the values of β and the rationalization of the system properties using MD calculation were performed at first for NMA–NMA. To this end the DL_POLY code⁴⁹ was used by adopting a NVE ensemble of particles (so as to ensure the conservation of total energy (E_{tot})) and imposing no boundary conditions. All simulations were initiated with the NMA–NMA geometry given in ref. 50 and the system was equilibrated for 10 ps. After achieving

equilibration, trajectories were further integrated for 1.5 ns using a time step of 0.1 ps.

Batches of calculations, starting from different initial configurations, were carried out at values of E_{tot} corresponding to temperatures of about 100 K. This was motivated by the wish of singling out the fingerprint of the formation of the various isomers and collecting evidence on the fact that at $T = 100$ K the system has enough energy to surmount the barriers separating the different conformers. Then the geometries of the most stable isomers were selected as initial configurations for further runs at decreasing values of E_{tot} (and consequently of T) in order to figure out a trend allowing a safe extrapolation of the temperature to 0 K (although this does not give an exact evaluation of the minimum potential energy value it provides a valid basis to speculate on it). As a matter of fact in our work we take as equilibrium geometry that of $T = 2$ K (the lowest studied temperature). In this perspective, the distributions of the relevant angles and distances along the trajectories were analyzed to assess whether the proposed equilibrium geometries correspond to limiting values of distances and angles. A careful inspection of the results has been performed also to assess whether the dynamical results correspond only to one conformer or to different conformers having similar energies by plotting the total potential energy, V , as a function of relevant distances. It is worth noticing here that, under the conditions of the present study, V is mainly affected by the behaviour of V_{vdW} and, therefore, the analysis is mainly focused on the dependence of the various features from the basic parameters of V_{vdW} . A typical plot of this type is given in Fig. 2, where the values of V calculated for two different simulations of NMA–NMA are shown to illustrate two opposite situations. Panel (a) shows the case in which only one conformer is formed whereas panel (b) shows the case in which more than one conformer is formed. In the first case

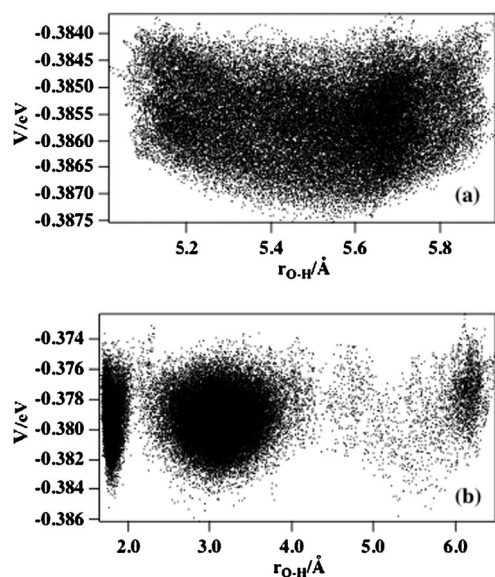


Fig. 2 Panel (a): simulations carried out at $T = 5$ K in which only one NMA–NMA conformer is formed. Panel (b): simulations carried out at $T = 15$ K in which different NMA–NMA conformers are formed.

(panel (a)), the values of V plotted as a function of the distance from the O of the carbonyl group to the H of the amide group (r_{OH} distance) end up to be grouped in a single interval while in the second case (panel (b)) the V values end up to be grouped in different intervals. This indicates that the same (or very similar) energy values can be associated to different geometries and accordingly to different conformers.

3.1 The interaction optimization

Ab initio calculations for the conformers of the NMA dimer, having different geometries and/or binding energies,^{12,13,28} are reported in the literature. For instance, Köddermann and Ludwig,²⁸ from density functional calculations at the B3LYP/6-31+G* level of theory, calculated a binding energy (D_e) of -27.84 kJ mol⁻¹ (-0.2885 eV) (-26.50 kJ mol⁻¹ (-0.2746 eV) when making a counterpoise correction). At the same time Vargas *et al.*,¹⁸ in their MP2/aug-cc-pVDZ level study aimed at optimizing the geometries *via* single-point calculations, finding lower binding energy values (-0.4193 eV at the best level of calculation that includes BSSE corrections). Other *ab initio* estimates of the interaction energy are reported in the literature. They differ in some cases^{18,51} up to about 60%. Despite this large difference one can clearly conclude that the NMA non-planar dimers are the most stable. It can also be concluded that higher is the level of the *ab initio* calculation larger is the interaction energy (weaker is the intermolecular binding). They also suggest -0.3 eV as a suitable reference value for the NMA dimer binding energy D_e .

Our MD calculations were carried out using the AMBER charge distribution for NMA and a value of 8 for β of all pairs (a value smaller than 9.0, the one adopted for rare gas dimers,³⁴ in agreement with that indicated in Section 2.2). The above mentioned *ab initio* estimates of the geometrical characteristics of the NMA dimer are reproduced by our MD calculations. They predict, in fact, as most stable a non-planar dimer geometry, in which the NMA monomers are not parallel to each other. Additional MD calculations were performed using the other two charge distributions proposed for NMA. Also in this case an initial value of $\beta = 8$ was adopted. Results show that AMBER distribution leads to the most stable dimer whereas the OPLS-AA distribution leads to the less stable one. This prompted an MD investigation on how different values of β can counterbalance the variation of the charge distributions. The MD calculations were repeated by varying the value of β (within the already mentioned limited range) to either soften or harden (see Section 2.1) the core repulsive wall (and change, accordingly also the corresponding attraction) as done in the past for pure water.²⁶ The search was driven by the attempt to reproduce the suggested dimer binding energy of about -0.3 eV for all the three mentioned charge distributions, because the reproduction of the equilibrium geometry seems to be scarcely sensitive to the variation of β . The optimized values of β obtained for the three charge distributions are given in Table 4. As can be seen from the table, in the AMBER case that we discuss first, the highest β value corresponds to the interaction between the effective N–H group and O (O–N pair).

Table 4 Values of the β parameters for the different effective pair interactions. X and Y indicate the R and L subindices (see Fig. 1)

Distrib/Pairs	C _X –C _Y	C–C	O–O	N–N	C _X –C	C _X –O	C _X –N	C–O	C–N	O–N
AMBER	8.0	8.0	8.0	8.0	8.0	8.0	8.0	8.0	8.0	8.8
CHARMM22	8.2	8.0	8.0	7.8	8.0	7.8	8.0	8.0	8.0	7.8
OPLS-AA	8.2	8.3	8.0	7.8	8.0	7.4	8.0	8.0	8.0	8.6

3.2 The NMA dimer properties

The MD calculations, performed using the AMBER charge distribution and the optimized β values shown in the first row of Table 4, singled out some peculiar structural properties of the two preferred geometries of the NMA dimer. In one of them, the oxygen atoms of the carbonyl group of both NMA molecules form H-bonds with one H of the CH₃ group (conformer A). In the other geometry, corresponding to a nearly perpendicular configuration, the O of the carbonyl group forms a H-bond with the H of the NH group, with a small additional contribution of the C=O...H(CH₃) (conformer B). Because of the higher number of H-bonds, conformer A is stabler than conformer B. The existence of conformers stabilized only by H-bonds, formed between methyl groups and O, is not surprising. Whitfield *et al.*¹⁹ in an analysis of joint distribution functions of the structural properties of liquid NMA observed that the getting into close distance (called contact by them) of O...H(CH₃) can be rationalized in two different ways. In one case, two molecules already connected by a traditional N–H...O=C hydrogen bond form an additional C=O...H(CH₃) hydrogen bond reinforcing in this way the pre-existing interaction. In the other case, the C=O...H(CH₃) hydrogen bond forms with no reference to a pre-existing N–H...O=C one. The authors point out that in this case the H-bonds are preferably formed between different chains of NMA molecules *via* the forming of a N–H...O=C hydrogen bond with a third NMA molecule.

Both conformers have been investigated using MD calculations and a sketch of their structure is shown in Fig. 3. Conformer A (left hand side (lhs) panel), has an interaction energy of –0.3507 eV and H-bond distances equal to 1.90 Å. Conformer B (right hand side (rhs) panel) has an interaction energy of –0.3123 eV and an equilibrium distance from the O to H...N of 1.84 Å. As is apparent from the right hand side panel of the figure, some cooperative effects between the C=O...H(CH₃) hydrogen bonds take place also in the conformer B, with the O...H distance being 2.70 Å. The cooperative effect of different hydrogen bonds in the stabilization of the *trans* NMA dimer has also been reported by other authors.^{18,13}

The equilibrium potential energy of each conformer has been derived as indicated before by an extrapolation to 0 K of results obtained in the range of *T* going from 15 K to 2 K. To compare our results with those of the bibliography, binding energies have been calculated by subtracting the energy of two fully optimized monomers from the energy of the dimer. The geometries of conformers of type A have not been explicitly described in the literature. Accordingly, in Table 5 we compare only the geometry and the energy values estimated for conformer B. These turned out to be similar to those reported in the literature (geometrical information given in the first row

Table 5 The values of binding energy, D_e , and selected geometry data for the NMA–NMA system.^a (Conformer B, see text and Fig. 5)

D_e /eV	$r_{OH}/\text{\AA}$	$r_{NO}/\text{\AA}$	$r_{O-H(CH_3)}/\text{\AA}$	$\widehat{NHO}/^\circ$	$\widehat{COH}/^\circ$	Reference
–0.3123	1.844	2.860	2.701	171.3	131.2	Present
–0.2550	—	3.028	—	—	—	Ref. 51
–0.2746	—	—	—	—	—	Ref. 28
–0.2888	2.01	2.97	—	157.0	122.0	Ref. 54
–0.3100	1.96	2.96	—	168.0	118.0	Ref. 54
–0.3452	1.85	—	—	180.0	168.0	Ref. 9
–0.3777	1.82	—	—	—	—	Ref. 55
—	1.956	2.952	—	179.6	133.6	Ref. 13
—	1.995	3.010	—	175.0	147.5	Ref. 13
—	2.183	3.195	—	172.3	148.9	Ref. 13
–0.4193	2.035	2.949	2.685	148.1	106.3	Ref. 18

^a AMBER charge distribution has been used to calculate the electrostatic interaction.

of Table 5 refers to the energy minimum of the 2 K simulation). To put the analysis on a more quantitative basis we consider here also some distances and angular distributions. For this reason the radial distribution of the N–H...O=C distances and the NHO and COH angular distributions of both conformers are shown in the top panel of Fig. 4. The figure shows that the maximum of the radial distribution for conformer B peaks at a small value of the N–H...O=C distance (that indicates the formation of a typical H-bond between amide molecules). In contrast, the maximum of the radial distribution for conformer A peaks at large N–H...O=C distances (that indicates in this case a lack of participation of H of the NH group in the formation of H-bonds).

The existence of more than one isomer allows an investigation of the isomerization process as a function of E_{tot} (or *T*). The MD calculations show that when the initial configuration is that of conformer B, the isomerization process begins at temperatures of about 30 K. This can be clearly seen from Fig. 5 where the values of *V* (lhs panels) and the two NH...O=C distances (see conformer B in Fig. 3) are plotted against the simulation time at temperatures of 10 K, 15 K and 30 K (from the top to the bottom panels). The Figure shows small changes on both the potential energy and the NH...O=C distances at the two lower temperatures. In contrast, at *T* = 30 K, conformer B isomerizes to conformer A as clearly indicated by the variation of *V* (lhs lower panel) and of the two NH...O=C distances (which become equal after differing for 0.3 ns at the beginning of the trajectory). The rhs lower panel of Fig. 5 gives also the more quantitative information that the shorter distance oscillates around a value of 1.9 Å while the largest one around a value of 6.4 Å (as typical of the equilibrium configuration of conformer B). The plots show also that at larger times they converge to a mean value of about 3.9 Å (as typical of the equilibrium configuration of conformer A) whereas, no further interconversions

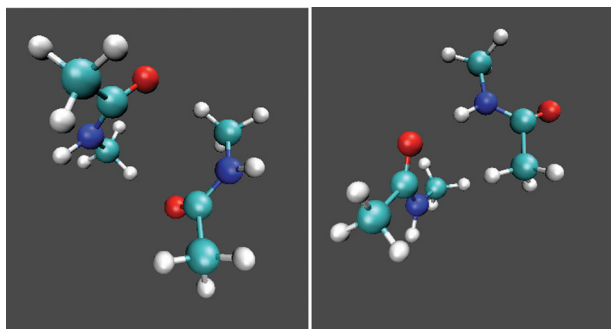


Fig. 3 Two conformers of the NMA dimer. On the left hand side panel, the most stable (conformer A) is shown for which the H-bonds are formed by the hydrogen atoms of the methyl groups. On the right hand side panel the less stable (conformer B) is shown for which the main contribution to the H-bond is $\text{N-H}\cdots\text{O}=\text{C}$. However, the contribution of the H-bond from an H of the methyl group is also appreciable.

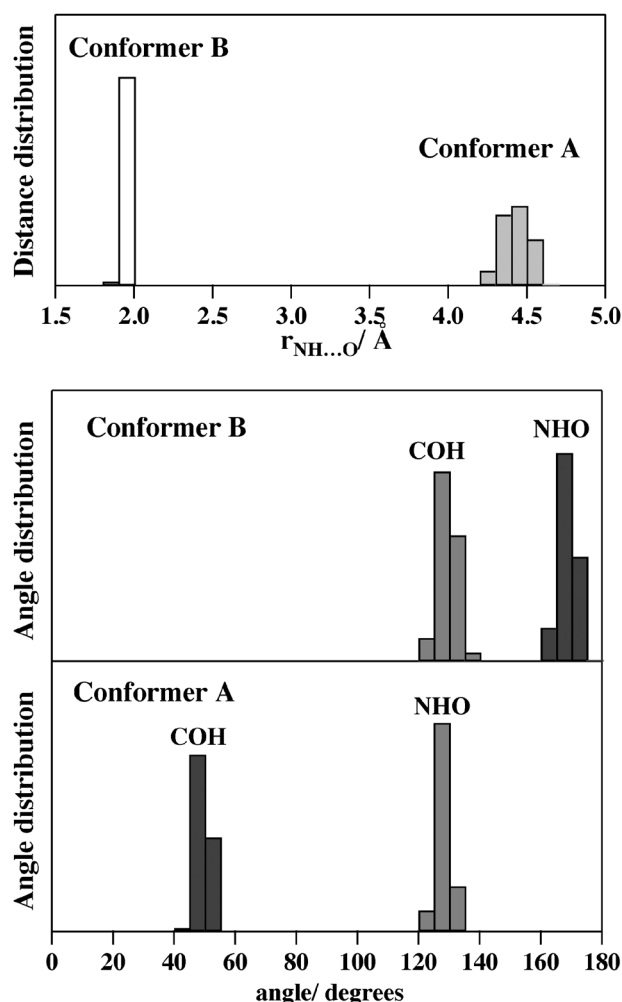


Fig. 4 Top panel: the distribution of the $r_{\text{NH}\cdots\text{O}}$ distances for conformers A and B. Central (conformer B) and bottom (conformer A) panels: the distributions of the NHO and COH angles. Calculations have been performed using AMBER charges and parameters in Tables 1 and 4.

are observed at longer times. The already mentioned other way of analysing the isomerization process is that of inspecting the

variation of V as a function of a properly chosen internuclear distance (like in Fig. 2). For instance, in Fig. 6, the values of V (top and central panels), sampled by a simulation performed at T below 30 K, are plotted as a function of the smaller $\text{NH}\cdots\text{O}=\text{C}$ distance that shows to be confined in the range 1.7–2.0 Å. This indicates that the A conformers are not formed during the considered simulation. However, a quite different result is obtained when T is increased to 30 K. In this case the sampled values of V group around two different values of the $\text{NH}\cdots\text{O}=\text{C}$ distances (respectively 1.9 Å (conformer B) and 4.0 Å (conformer A)).

4. The porting of the model potential MD calculations

To investigate the porting of the proposed model potential to other situations, additional extended MD calculations have been performed both for the NMA–NMA and the NMA– H_2O systems. The characteristics of the simulations are the same as indicated in the previous section. Moreover, as indicated before, for the NMA–NMA system the calculations have been extended to different charge distributions. In this case, in order to obtain acceptable results when trying to predict the existence of conformer B (as already mentioned information on conformer A are too limited) using CHARMM22 and OPLS-AA charge distributions, the possibility of using β values differing from the AMBER optimal ones has been considered. The study of the NMA– H_2O clusters was instead targeted to better understand the hydration mechanisms and to further explore the physical implications of varying the β parameter.

4.1 The effect of changing the charge distribution

The CHARMM22 and the OPLS-AA charge distributions considered in our investigation differ from the AMBER one (see Table 4) mainly for the value assigned to the punctual charges (not for their location, as already mentioned in the previous section) attached to the H atoms located on the methyl group close to $\text{NH}(\text{C}_\text{R}\text{H}_3)$. Accordingly, the AMBER value (0.1127 a.u.) is higher than the CHARMM22 and OPLS-AA ones (which are 0.09 a.u. and 0.06 a.u. respectively). The higher value of the H charges in AMBER favours the interaction between O and $\text{C}_\text{R}\text{H}_3$. Moreover, also the charge of -0.5911 a.u. placed by AMBER on the O atom is higher, in absolute value, than those of CHARMM22 (-0.51 a.u.) and of OPLS-AA (-0.50 a.u.). At the same time, the value of the binding energies obtained with CHARMM22 and OPLS-AA charge distributions is higher than the AMBER one, as a result of the associated weaker V_{el} . Such difference can be reconducted to the contribution of $\text{NH}\cdots\text{O}=\text{C}$ that is the main contributor to the stability of conformer B. In this respect, the AMBER distribution leads to a value of the product of the oxygen and H (of the NH group) charges that in absolute value is larger than that of CHARMM22 and OPLS-AA. This means that the AMBER scheme generates a more attractive electrostatic interaction. Moreover, the model predicts for CHARMM22 a value of D_{e} equal to -0.2492 eV and $\text{NH}\cdots\text{O}=\text{C}$ and $\text{C}=\text{O}-\text{H}(\text{CH}_3)$ distances equal to 1.887 Å and 2.346 Å, respectively, while for OPLS-AA it predicts a binding energy of -0.2147 eV and $\text{NH}\cdots\text{O}=\text{C}$ and

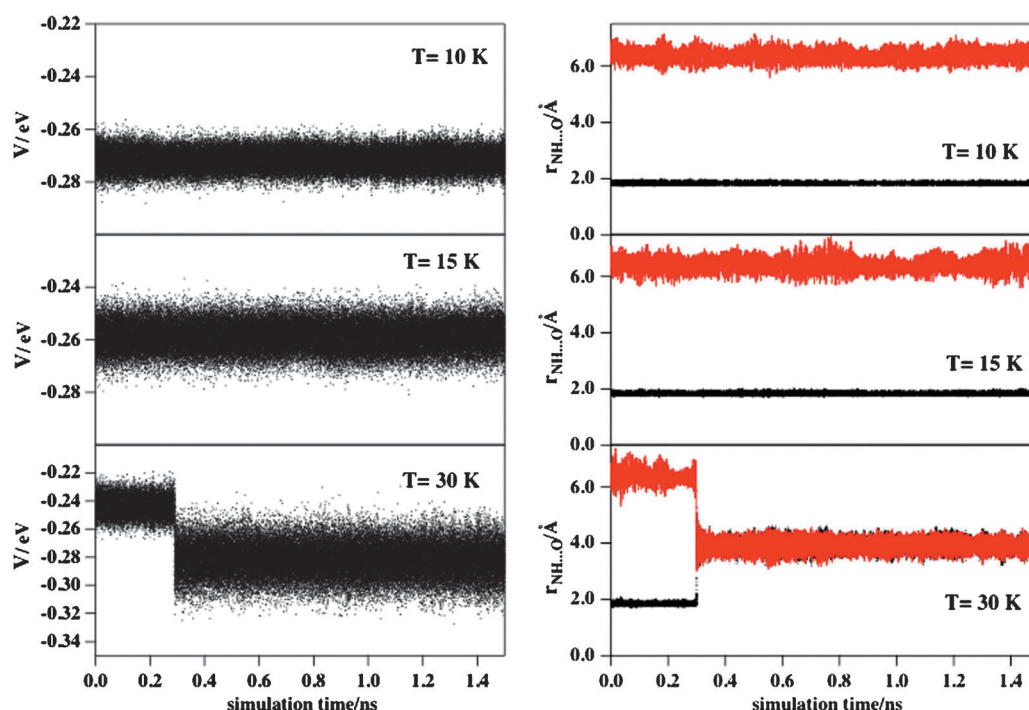


Fig. 5 Evolution of the total potential energy, V (left hand side), and of the N-H...O=C distances, $r_{\text{NH}\cdots\text{O}}$ (right hand side), with the simulation time for three values of T .

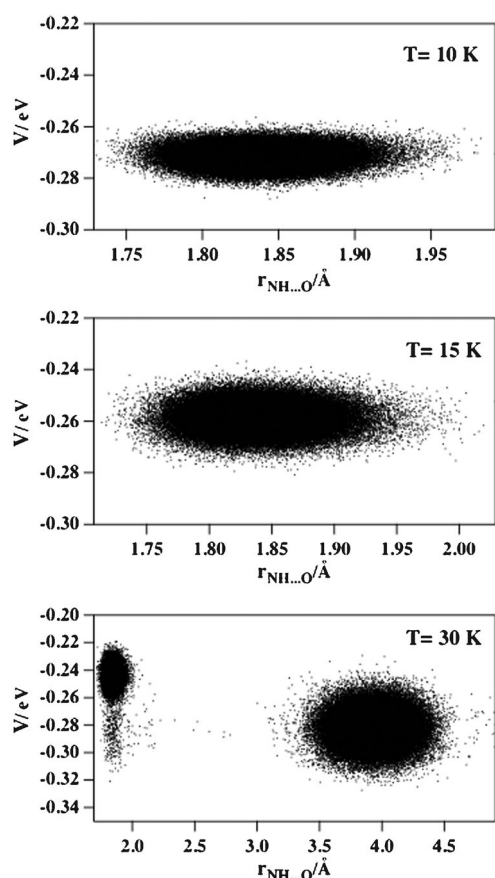


Fig. 6 Evolution of the total potential energy, V , as a function of one of the N-H...O=C distances, $r_{\text{NH}\cdots\text{O}}$, at three values of T .

C=O-H(CH₃) distances of 1.914 Å and 2.473 Å, respectively. The calculated values of the binding energy are higher than those quoted in Table 5. Actually, using the β values optimized for the AMBER charges, it has been found that the binding energies follow, in general, the sequence: $(D_e)_{\text{AMBER}} \approx 1.22$ $(D_e)_{\text{CHARMM22}} \approx 1.36$ $(D_e)_{\text{OPLS-AA}}$.

The lower attractive component associated with the CHARMM22 and OPLS-AA distributions can be partially compensated, as shown in the study of the adaptability of the V_{ILJ} formulation,²⁶ by a corresponding decrease of the repulsive component of V_{vdW} . This compensation has been achieved by lowering the β value of the (N-H) ··· O pair and by evaluating its effect both on the binding energy D_e and on the length of the NH...O=C distance. For the CHARMM22 charge distribution this can be understood with the help of Table 6, in which the values of the binding energy and selected geometry information for different values of $\beta_{\text{O-N}}$ are shown. As expected, lower values of $\beta_{\text{O-N}}$ give lower values of the D_e and therefore increase the dimer stability. As expected, no noticeable changes in the

Table 6 The values of the binding energy, D_e , and selected geometry data for different β values for the NMA-NMA dimer (conformer B)^a

$\beta_{\text{O-N}}$	D_e/eV	$r_{\text{OH}}/\text{\AA}$	$r_{\text{NO}}/\text{\AA}$	$r_{\text{O-H(CH}_3\text{)}}/\text{\AA}$	$\widehat{\text{NHO}}/^\circ$	$\widehat{\text{COH}}/^\circ$
8.8	-0.2492	1.887	2.346	2.981	163.3	132.5
8.5	-0.2566	1.885	2.374	2.881	164.3	132.0
8.2	-0.2616	1.883	2.401	2.883	164.4	132.3
8.0	-0.2631	1.859	2.367	2.863	166.1	130.3
7.8	-0.2670	1.821	2.396	2.827	167.7	131.4

^a CHARMM22 charge distribution has been used to calculate the electrostatic interaction.

Table 7 The values of the binding energy, D_e , and selected geometry data for the NMA–NMA dimer (conformer B)

	D_e/eV	$r_{\text{OH}}/\text{\AA}$	$r_{\text{NO}}/\text{\AA}$	$r_{\text{O}-\text{H}(\text{CH}_3)}/\text{\AA}$	$\widehat{\text{NHO}}/^\circ$	$\widehat{\text{COH}}/^\circ$
^a	−0.2748	1.836	2.840	2.367	166.5	130.5
^b	−0.2575	1.854	2.860	2.449	166.6	130.6

^a CHARMM22. ^b OPLS-AA charge distributions (see the text).

NMA–NMA geometry are observed when lowering $\beta_{\text{O-N}}$ from 8.8 to 8.2. However, by further lowering $\beta_{\text{O-N}}$, the $\text{NH}\cdots\text{O}=\text{C}$ distance decreases to very low values. The same behaviour has been observed for the OPLS-AA charge distribution. To allow a decrease of the binding energy without decreasing the $\text{NH}\cdots\text{O}=\text{C}$ distance also other β values were slightly varied (see Table 4).

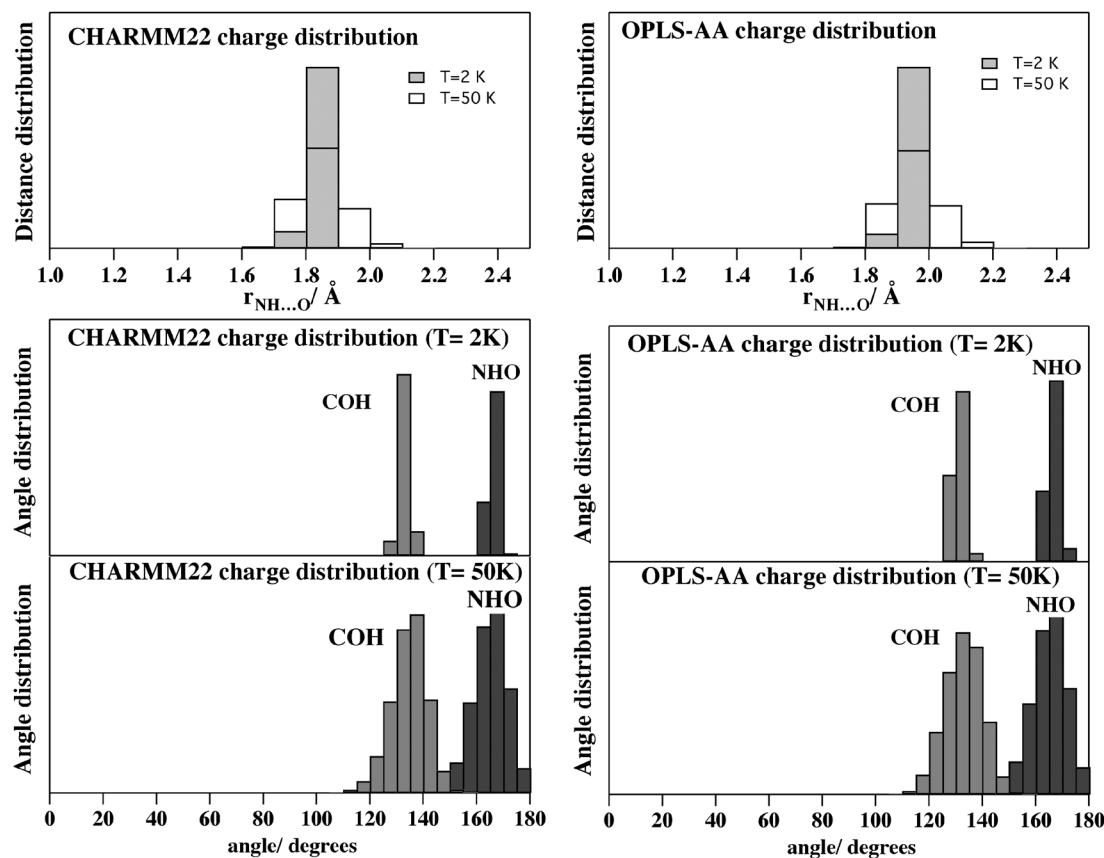
The resulting values of the binding energy and geometrical parameters, using the β values given in the second row of Table 4, are given in Table 7. They confirm the scarce sensitivity of the geometries to the variation of the binding energy (that varies only of about 6%) and still fall within the higher limit of the values shown in Table 5. These results confirm also that higher is the level of the *ab initio* calculations larger is the value of the calculated D_e (the uncertainty of *ab initio* values has clear consequences on the optimization of β).

The MD calculations performed using CHARMM22 and OPLS-AA distributions singled out that, once β is optimized, the results obtained at the temperatures considered (see Fig. 7)

do not differ significantly from those obtained when using the AMBER charges (see medium panel of Fig. 4).

4.2 The effect of hydration

Most of the theoretical studies of NMA–H₂O reported in the literature focus on the H-bond interaction using *ab initio* calculations and single out three different conformeric structures: (I) the O of the carbonyl group and the hydrogen atom of water (Hw) forming an H-bond with the H₂O molecule oriented towards the C_LH₃ group (see Fig. 1), (II) the O of the carbonyl group and Hw forming an H-bond with the H₂O molecule oriented towards the C_RH₃ group (see Fig. 1) and (III) the H of the NH group forming an H-bond with the oxygen atom of water (Ow) (see for instance ref. 10 and 50). However, some authors do not make distinction between conformers I and II (in which one Hw is bonded with the O atom of the carbonyl group) while they make a clear difference between conformer III (in which the H-bond is formed between the amide group and Ow^{9,28}) and the others. The similarity between conformers I and II is due to the fact that they are both stabilized by H bonds formed by the O atom of the carbonyl group and one of the H atoms of the water, leading to similar binding energies, $\text{HOH}\cdots\text{O}=\text{C}$ distances and OHO and COH angles.¹⁰ Some authors calculate differences in the related binding energies to amount only to 0.008 eV⁵⁰ (or to be even nul) when increasing the level of *ab initio* calculations.^{10,52}

**Fig. 7** The distribution of the $r_{\text{NH}\cdots\text{O}}$ distances and NHO and COH angles corresponding to CHARMM22 (lhs) and OPLS-AA (rhs) charge distributions when using the ILJ parameters in Tables 1 and 4.

For this reason our calculations focused on the NMA–H₂O conformer III to optimize the values of β for the three charge distributions already considered for NMA–NMA. Moreover, one has to take into account that while the dipole moment of water in the gas phase is equal to 1.85 D, the increase of charge transfer, induction (polarization) and many-body effects generated by the proximity of NMA to H₂O makes the dipole moment of water larger than that of the water monomer.⁵³ As proposed previously,⁴⁶ in our calculations an initial value of μ equal to 2.1 D as for the water dimer³² was considered.

By considering $\mu = 2.1$ D and optimizing the values of β ($\beta = 8.0$ for N–Ow and $\beta = 8.5$ for C_X–Ow, C_Y–Ow and O–Ow, Table 4) satisfactory predictions of the NMA–H₂O binding energies were obtained for all the three different NMA charge distributions (see Table 8) by extrapolating the binding energies calculated at several temperatures down to $T = 0$ K (as done also for NMA–NMA). It is worth noticing here that, as shown in Table 9 for the AMBER charge distribution, although the β values have been optimized for conformer III (in which NMA and H₂O interacts through the NH··Ow bond) the use of the same values of β still predicts the main characteristics (energy and geometry) of conformer II (even if it interacts mainly through an C=O··Hw bond).

As already found before, the AMBER charge distribution leads again to the higher estimate of the stability of the conformers and, accordingly, to the lower estimate of the binding energy. At the same time the other two charge distributions, which provide approximately the same value of the NMA dipole moment, lead to more similar binding energies. The binding energies calculated for conformers II and III are comparable with DFT results of -0.3410 eV and -0.2359 eV, respectively, obtained at the B3LYP/6-31+G* level (without counterpoise corrections).²⁸ Higher theoretical values have been obtained when adding counterpoise

corrections (-0.3119 eV and -0.1984 eV for conformers II and III, respectively).

In our calculations the interplay between the values of β and μ has been further investigated because, as already pointed out for the H₂O dimer,²⁶ the variation of β may, at least partially, compensate also for the differences originated from the use of different charge distributions (though in certain cases an increase of β is unable to sufficiently increase the value of the binding energy). Binding energy values shown in Table 8 indicate that when the NMA AMBER charge distribution is used, the potential function is largely attractive. The attractive character of the potential function can be efficiently modified not only by varying the charge distribution of NMA but also changing that of water, *i.e.* by reducing its dipole moment value. The effect of varying μ was investigated using the dipole moment of the water monomer in the gas phase (1.85 D). With $\mu = 1.85$ D, the value of the binding energy of conformers II and III becomes equal to -0.3167 eV and -0.2167 eV, respectively. These energy values, together with selected geometry information, are given in Table 9 where they are compared with results quoted from the literature. Some radial and angular distributions calculated at 2 K using a water dipole moment of 1.85 D are shown in Fig. 8. Results for conformer II are given in the left hand side panels of the figure, while those of conformer III are given in the right hand side ones. As can be seen from the top left hand side panel of the Figure, the distribution of the CO··Hw distances peaks at a value of 1.85 Å, while the largest COHw and NH₂Ow angle populations correspond to values of 135° and 175° respectively. In the right hand side panels of Fig. 8, instead, the most populated NH··Ow distance is shown to correspond to a distance of 2.05 Å, and a NH₂Ow angle of about 175°.

5. Concluding remarks

In this paper a recently proposed intermolecular potential model based on the additivity of polarizability components has been applied to the NMA–NMA and the NMA–H₂O intermolecular aggregates. The potential is formulated as a set of coulombic terms plus a set of V_{ILJ} contributions assigned to various interaction centres and properly placed on each molecule

Table 8 The values of NMA–H₂O binding energies of conformers II and III in eV

NMA charges	AMBER	CHARMM22	OPLSAA
Conformer II	−0.3498	−0.2927	−0.2836
Conformer III	−0.2404	−0.2394	−0.2298

Table 9 The values of binding energy, D_e , and selected geometry data for the NMA–H₂O system. Results on the two first rows have been calculated using the NMA AMBER charges and a dipole moment of 1.85 D for H₂O

Conformer	D_e /eV	$r_{OH}/\text{\AA}$	$\widehat{NH\!Ow}/^\circ$	$\widehat{OH\!wOw}/^\circ$	$\widehat{COHw}/^\circ$	Reference
II	−0.3167	1.8430	177.16	—	—	Present
III	−0.2167	2.0130	—	175.6	135.4	Present
I	−0.4250	1.8758	—	174.92	135.30	Ref. 10 ^a
	(−0.3166)	(1.9878)	—	(176.83)	(135.09)	
II	−0.4163	1.8800	—	165.07	115.89	Ref. 10 ^a
	(−0.3166)	(1.9813)	—	(168.37)	(115.37)	
III	−0.3252	1.9933	176.84	—	—	Ref. 10 ^a
	(−0.2342)	(2.1246)	(176.91)	—	—	
II	−0.3410	—	—	—	—	Ref. 28 ^b
	(−0.3119)	—	—	—	—	
III	−0.2359	—	—	—	—	Ref. 28 ^b
	(−0.1984)	—	—	—	—	

^a HF/6-31G (without parentheses), HF/6-31G* (in parentheses). ^b Without counterpoise correction (without parentheses), with counterpoise correction (in parentheses).

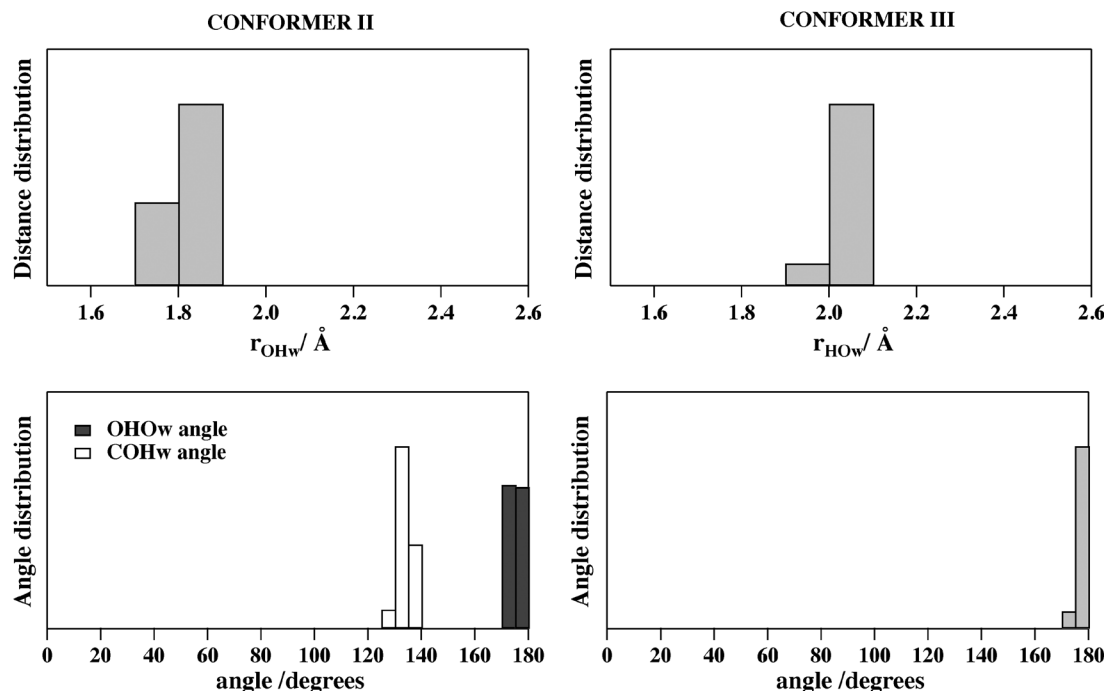
water: $\mu = 1.85$ D, NMA: AMBER charges

Fig. 8 Radial and angular distributions for conformers II and III. NMA AMBER charges and the dipole moment of a water monomer in a gas phase have been used in the calculations.

of the aggregate. The ϵ and r_0 pairs of parameters of the V_{ILJ} terms have a structural nature. Accordingly their values were ported among the various involved interaction pairs. The remaining parameters embody more delocalized contributions whose values were, therefore, optimized to render the pair components of more collective contributions like hydrogen bonding, particle clustering and dipole moments.

The resulting machinery has been incorporated in a MD treatment. This has made it possible to reproduce some (theoretical and experimental) properties of the NMA–NMA and the NMA–H₂O systems and to rationalize their origin. For this purpose different charge distributions, for the intervening molecules, have been considered and the relative role played by β and μ has been investigated. The interplay of β and μ values was found to be fundamental to preserve the transferable nature of the structural parameters. In particular, for NMA–NMA, the investigation has been performed by adopting the more convenient set of β values for each of the different NMA charge distributions considered while for NMA–H₂O a single set of β values was instead considered.

NMA–NMA results show that the V_{ILJ} function (through the modulation of β) adds enough flexibility to the van der Waals interaction to cope with different electrostatic environments without changing the structural parameters, ϵ and r_0 , of the various pair potentials. The investigation of the NMA–NMA interactions shows also that all the three charge distributions predict the existence of a conformer B having similar geometrical characteristics and binding energies, whose values can be rationalized in terms of the corresponding charge distributions. The results show that the C=O–H(CH₃) hydrogen bond, relevant to biological systems, can play an important

stabilizing role when conformer B is formed.¹⁹ From the structural investigation of such a conformer, it has been observed that, in general, the N–H...O=C distance falls at the lower limit of the results available in the literature. Attempts to increase this distance led to an increase of the binding energy and make the conformers less stable. Moreover, conformer A, in which the typical NH...O=C peptide bond is not formed, is only observed when AMBER charges are used. This conformer shows the tendency to give interchain contacts which allow the NMA to interact either with other dimers or with single NMA molecules through a NH...O bond.

NMA–H₂O results show that a single set of β parameters is able to describe the main characteristics of the interaction. The model predicts the existence of two conformers. In one of them the oxygen of the carbonyl group and an hydrogen atom of water participate in the formation of the H-bond. This conformer (conformer II) is also stabilized by a weaker H-bond than the O atom of water forms with hydrogens of the C_LH₃ methyl group (see Fig. 1). The other conformer (conformer III) is characterized by the formation of the typical amide H-bond (between the H of the NH group and the O of water). The higher stability of both conformers is predicted when the NMA AMBER charge distribution is used, with the prediction of the binding energy falling in the lower limit of the values reported in the literature. The role played by the dipole moment of water has been investigated and the binding energy values of NMA–H₂O conformers have been improved by lowering the dipole moment of water from 2.1 D to 1.85 D.

A comparison of NMA–NMA and NMA–H₂O results indicates that the interaction of the former is more sensitive to the values of β than that of the latter. The higher sensitivity

of the NMA–NMA interactions to the β values has been found to be associated with the higher number of effective pair interactions (with respect to that of NMA–H₂O) and their higher cooperative effect.

In general, it has been observed that the three NMA charge distributions used together with the V_{ILJ} function predict results in reasonable agreement with available data for both the NMA–NMA and NMA–H₂O dimers. This might imply that also other charge distributions could be supported by a proper assessment of the β parameters. To further validate this conclusion, the investigation is being extended to NMA solvated in a realistic aqueous environment, using an appropriate value of the dipole moment.

Acknowledgements

M. Albertí acknowledges financial support from the Ministerio de Educación y Ciencia (Spain, Project CTQ2010-16709). Thanks are also due to the Centre de Supercomputació de Catalunya CESCA-C4 and Fundació Catalana per la Recerca for the allocated supercomputing time. M. Albertí also acknowledges financial support from the Ministerio de Ciencia e Innovación (Spain, Mobility Program, Project PR2008-0251). F. Pirani and A. Laganà acknowledge financial support from the Italian Ministry of University and Research (MIUR) for PRIN Contract and EGI for the use of the grid segment available to the COMPChem VO.

References

- I. M. Klotz and J. S. Franzen, *J. Am. Chem. Soc.*, 1962, **84**, 3461.
- J. L. Katz and B. Pst, *Acta Crystallogr.*, 1960, **13**, 624.
- K. Itoh and T. Shimanouchi, *Biopolymers*, 1967, **5**, 921.
- F. Fillaux and C. De Loze, *Chem. Phys. Lett.*, 1976, **39**, 547.
- F. Fillaux and M. H. Baron, *Chem. Phys.*, 1981, **62**, 275.
- M. T. Zanni, M. C. Asplund and R. M. Hochstrasses, *J. Chem. Phys.*, 2001, **114**, 4579.
- S. Woutersen, Y. Mu, G. Stock and P. Hamm, *Chem. Phys.*, 2001, **266**, 137.
- J. R. Schmidt, S. A. Corcelli and J. L. Skinner, *J. Chem. Phys.*, 2004, **121**, 8887.
- M. Buck and M. Karplus, *J. Phys. Chem. B*, 2001, **105**, 11000.
- H. Guo and M. Karplus, *J. Phys. Chem.*, 1992, **96**, 7273.
- J. W. Caldwell and P. A. Kollman, *J. Phys. Chem.*, 1995, **99**, 6208.
- B. Mannfors, N. G. Mirkin, K. Palmo and S. Krim, *J. Comput. Chem.*, 2001, **22**, 1933.
- T. M. Watson and J. D. Hirst, *J. Phys. Chem. A*, 2002, **106**, 7858.
- K. Kwac and M. Cho, *J. Chem. Phys.*, 2003, **119**, 2247.
- M. Kank and P. E. Smith, *J. Comput. Chem.*, 2006, **27**, 1477.
- S. K. Allison, S. P. Bates, J. Crain and G. J. Martyna, *J. Phys. Chem. B*, 2006, **110**, 21319.
- Z. Z. Yang and P. Qian, *J. Chem. Phys.*, 2006, **125**, 064311.
- R. Vargas, J. Garza, R. A. Friesner, H. Stern, B. P. Hay and D. A. Dixon, *J. Phys. Chem. A*, 2001, **105**, 4963.
- T. W. Whitfield, J. Crain and G. J. Martyna, *J. Chem. Phys.*, 2006, **124**, 094503.
- J. Wang, P. Cieplak and J. Kollman, *J. Comput. Chem.*, 2000, **21**, 1049.
- A. D. MacKerell Jr., D. Bashford, M. Bellott, R. L. Dunbrack, Jr., J. D. Evanseck, M. J. Field, S. Sischer, J. Gao, H. Guo, S. ha, J. McCarty, L. Kuchnir, K. Kuczera, F. T. K. Lau, C. Mattos, S. Michnick, T. Ngo, D. T. Nguyen, B. Prodhom, W. E. Reiher III, B. Roux, M. Schlenkrich, J. C. Smith, R. Stote, J. Straub, M. Watanabe, Wiórkiewicz-Kuczera, D. Yin and M. Karplus, *J. Phys. Chem. B*, 1998, **102**, 3586.
- W. L. Jorgensen, D. S. Maxwell and J. Tirado-Rives, *J. Am. Chem. Soc.*, 1996, **118**, 11225.
- J. Hermans, H. J. C. Berendsen, W. F. van Gunsteren and J. P. M. Postma, *Biopolymers*, 1984, **23**, 1513.
- W. D. Cornell, P. Cieplak, C. I. Bayly, I. R. Gould, K. M. Merz Jr., D. M. Ferguson, D. C. Spellmeyer, T. Fox, J. W. Caldwell and P. A. Kollman, *J. Am. Chem. Soc.*, 1995, **117**, 5179.
- P. E. Mason and J. W. Brady, *J. Phys. Chem. B*, 2007, **111**, 5669.
- N. Faginas Lago, F. Huarte Larrañaga and M. Albertí, *Eur. Phys. J. D*, 2009, **55**, 75.
- M. Albertí, A. Castro, A. Laganà, M. Moix, F. Pirani, D. Cappelletti and G. Liuti, *J. Phys. Chem. A*, 2005, **109**, 2906.
- T. Köddermann and R. Ludwig, *Phys. Chem. Chem. Phys.*, 2004, **6**, 1867.
- S. Ataka, H. Takeuchi and M. Tasumi, *J. Mol. Struct.*, 1984, **113**, 147.
- M. Albertí, A. Aguilar, M. Bartolomei, D. Cappelletti, A. Laganà, J. M. Lucas and F. Pirani, *Lect. Notes Comput. Sci.*, 2008, **5072**, 1026.
- M. Albertí, A. Aguilar, D. Cappelletti, A. Laganà and F. Pirani, *Int. J. Mass Spectrom.*, 2009, **280**, 50.
- M. Albertí, A. Aguilar, M. Bartolomei, D. Cappelletti, A. Laganà, J. M. Lucas and F. Pirani, *Phys. Scr.*, 2008, **78**, 058108.
- F. Pirani, M. Albertí, A. Castro, M. Moix and D. Cappelletti, *Chem. Phys. Lett.*, 2004, **394**, 37.
- P. Pirani, S. Brizi, L. F. Roncaratti, P. Casavecchia, D. Cappelletti and F. Vecchiocattivi, *Phys. Chem. Chem. Phys.*, 2008, **10**, 5489.
- M. Albertí, A. Castro, A. Laganà, F. Pirani, M. Porriani and D. Cappelletti, *Chem. Phys. Lett.*, 2004, **392**, 514.
- M. Albertí, *J. Phys. Chem. A*, 2010, **114**, 2266.
- M. Albertí, A. Aguilar, J. M. Lucas, F. Pirani, D. Cappelletti, C. Coletti and N. Re, *J. Phys. Chem. A*, 2006, **110**, 9002.
- M. Albertí, A. Aguilar, J. M. Lucas, D. Cappelletti, A. Laganà and F. Pirani, *Chem. Phys.*, 2006, **328**, 221.
- M. Albertí, A. Castro, A. Laganà, M. Moix, F. Pirani and D. Cappelletti, *Eur. Phys. J. D*, 2006, **38**, 185.
- M. Albertí, A. Aguilar, J. M. Lucas, F. Pirani, C. Coletti and N. Re, *J. Phys. Chem. A*, 2009, **113**, 14606.
- M. Albertí, A. Aguilar, J. M. Lucas and F. Pirani, *Theor. Chem. Acc.*, 2009, **123**, 21.
- M. Albertí, A. Aguilar and F. Pirani, *J. Phys. Chem. A*, 2009, **113**, 14741.
- F. Huarte-Larrañaga, A. Aguilar, J. M. Lucas and M. Albertí, *J. Phys. Chem. A*, 2007, **111**, 8072.
- M. Albertí, A. Aguilar, J. M. Lucas and F. Pirani, *J. Phys. Chem. A*, 2010, **114**, 11964.
- F. Pirani, D. Cappelletti and G. Liuti, *Chem. Phys. Lett.*, 2001, **350**, 286.
- J. K. Gregory, D. C. Clary, K. Liu, M. G. BrOwN and R. J. Saykally, *Science*, 1997, **275**, 4705.
- M. Albertí, A. Aguilar, J. M. Lucas, F. Pirani, C. Coletti and N. Re, *J. Phys. Chem. A*, 2009, **113**, 14606.
- M. Capitelli, D. Cappelletti, G. Colonna, C. Gorse, A. Laricchiuta, G. Liuti, S. Longo and F. Pirani, *Chem. Phys.*, 2007, **338**, 62.
- http://www.cse.scitech.ac.uk/ccg/software/DL_POLY/ (last visited 15 June 2010).
- R. Zhang, H. Li, Y. Lei and S. Han, *J. Mol. Struct.*, 2004, **693**, 17.
- S. Trabelsi, M. Bahri and S. Nasr, *J. Chem. Phys.*, 2005, **122**, 024502.
- D. A. Dixon, K. D. Dobbs and J. J. Valentini, *J. Phys. Chem.*, 1994, **98**, 13435.
- K. Liu, M. G. BrOwN and R. Saykally, *J. Phys. Chem. A*, 1997, **101**, 8995.
- W. Qian, N. G. Mirkin and S. Krimm, *Chem. Phys. Lett.*, 1999, **315**, 125.
- W. L. Jorgensen, E. M. Duffy, J. W. Essex, D. L. Severance, J. F. Blake, N. A. McDonald and J. Tirado-Rives, *Computational Studies of Molecular Recognition from alkane dimers to protein–ligand complexes*, in *Crystal Engineering: The Design and Application of Functional Solids*, ed. K. R. Seddon and M. Zaworotko, Nato Series. Series C: Mathematical and Physical Sciences, 1996, vol. 539, p. 113.